Taylor & Francis
Taylor & Francis Group

Check for updates

The performance of collars on scour reduction at tandem piers aligned with different skew angles

Sargol Memar[a,b] , Mohammad Zounemat-Kermani[a] , Aliasghar Beheshti[c] , Majid Rahimpour[a] , Giovanni De Cesare[b] and Anton J. Schleiss[b]

[a]Water Engineering Department, Shahid Bahonar University of Kerman, Kerman, Iran; [b]Laboratory of Hydraulic Constructions (LCH), École Polytechnique Fédérale de Lausanne (EPFL), Lausanne, Switzerland; [c]Water Resources Engineering Department, Ferdowsi University of Mashhad, Iran

ABSTRACT

Local scouring is a leading cause of bridge collapses. To protect bridges against local scouring, different countermeasures have been proposed and tested in the literature. In this study, the performance of collars was evaluated for scour reduction at two tandem piers aligned with four skew angles (θ) of $0°, 30°, 60°, 90°$ with respect to flow direction. For this purpose, long duration tests were conducted with uniform sediments under clear-water conditions with flow intensities close to the threshold of sediment motion. The results showed that increasing the skew angle increased the scour depth, while the performance of collars for scour reduction decreased. The maximum and minimum scour depths occurred at skew angles of $\theta = 60°$ and $\theta = 0°$, respectively, around both the piers with and without collars. Analysis of the results indicated that the maximum scour depth at the upstream pier shifted to the downstream pier from $\theta \geq 20°$ and $\theta \geq 28°$ for the tandem piers with and without collars, respectively. In addition, as the skew angle increased, the equilibrium time of scour increased. Moreover, the performance of collars for scour reduction around the piers decreased over time.

Introduction

Flood conditions may cause major devastation to bridge foundations at river crossings. A hazard assessment of local scour at bridges for preventing bridge collapses has been progressively surveyed by many researchers. The main objective of scour countermeasures is the reduction of a scour hole around bridge piers. Classifying types of scour reduction techniques at bridge piers is attributed to the performance of scour protection devices against local scour. Techniques for scour reduction include flow-altering countermeasures and bed-armoring countermeasures. Flow-altering countermeasures, such as collars, sacrificial piles, bed sills, and submerged vanes, diminish the intensity of downflow and horseshoe vortices around bridge piers. However, bed-armoring countermeasures such as riprap stones, gabion, cabled-tied blocks, and geo-bags are placed at the base of piers as obstructions against scouring (Zarrati, Nazariha, and Mashahir 2006; Tafarojnoruz, Gaudio, and Calomino 2012).

Scour mechanism around bridge piers

The mechanism of scouring at bridge piers is a complicated process. The key factor for developing a scour hole is the existence of a complex vortex system produced at bridge piers. Due to the interaction of the approach flow with the pier face, a vertical flow forms on the leading face of the pier, which is distributed to up-flow and downflow jets. The up-flow moves toward the water surface and produces a bow wave. The downflow affects the streambed, creating a scour hole in front of the pier, and rolls up to generate a horseshoe vortex. The horseshoe vortex develops the scour hole until the bed shear stress becomes smaller than the critical bed shear stress. The separation of the approach flow on the sides of the pier produces the vortex shedding, forming wake vortices at the rear of the pier. Wake vortices are shed alternatively and move the sediment grains downstream through bed load and suspended load. Instantaneously, a combination of the horseshoe and wake vortices accelerates the scouring rate and the potential sediment transportation at the rear of the pier (Guo et al. 2012) (see Figure 1a).

At two tandem piers, sheltering and reinforcement effects are additional factors influencing scour depth at the piers. The sheltering effect is caused by the presence of the upstream pier and reduces the approach velocity toward the downstream pier. Thus, the strength of downflow and horseshoe vortices is reduced, and consequently, the scouring rate at the downstream pier becomes less than that at the upstream pier. As the streambed between the piers is
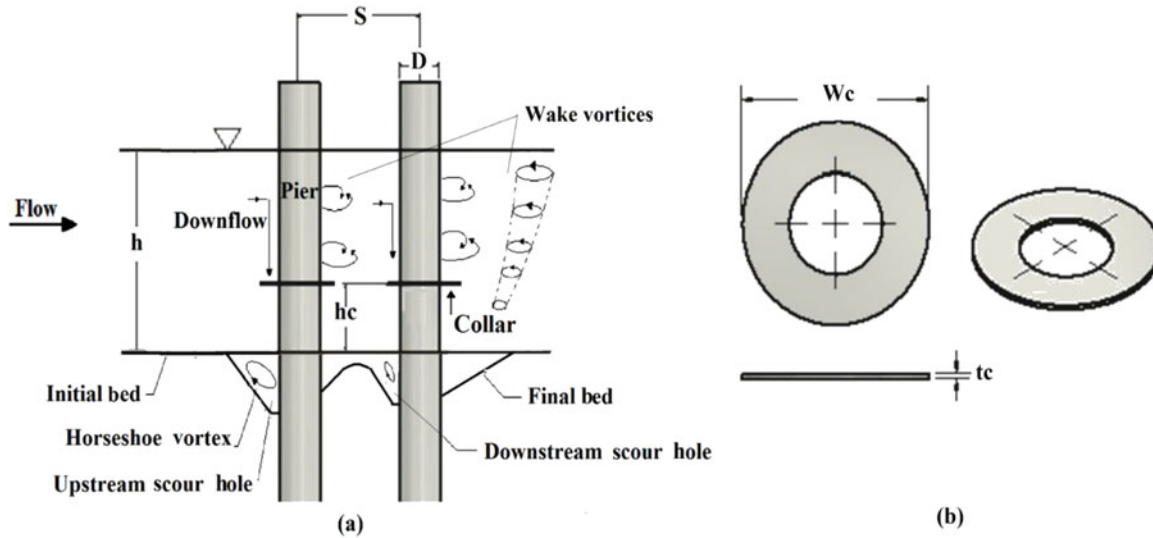

Figure 1. Flow pattern, scour holes and geometric parameters of tandem piers protected by collars for the skew angle of $\theta = 0°$ (a), Collar (b).

flattened, the mobility of the upcoming sediment grains from around the upstream pier may be facilitated, thereby, increasing the scour depth at the upstream pier (Zarrati, Nazariha, and Mashahir 2006; Lança et al. 2013).

Local scour at pier groups has been reported by several researchers in the past (Ataie-Ashtiani and Beheshti 2006; Arneson et al. 2012 (HEC-18); Lança et al. 2013; Beg and Beg 2015; Liang et al. 2017; Yilmaz, Yanmaz, and Koken 2017; Amini and Solaimani 2018; Liang, Wang, and Yu 2018). Ataie-Ashtiani and Beheshti (2006) derived a correction factor for estimating the maximum scour depth at pier groups. Amini and Mohammad (2017) presented a new approach to predict the scour depth at complex bridge piers. Amini and Solaimani (2018) investigated the influence of uniform and nonuniform pier spacing variations on scour depth at pier groups. Yilmaz, Yanmaz, and Koken (2017) developed a semi-empirical model to estimate the temporal evolution of scour depth at two tandem piers under clear-water conditions.

Local scouring at two bridge piers has been addressed in different numerical and experimental studies (Hannah 1978; Beg 2004; Selamoglu, Yanmaz, and Koken 2014; Kim et al. 2014; Wang et al. 2016; Hamidi and Siadatmousavi 2017; Khaple et al. 2017; Keshavarzi et al. 2018). Hannah (1978) observed maximum scour depth at two tandem piers for a pier spacing with a value $s = 2.5D$, where D is the pier diameter. Ataie-Ashtiani and Beheshti (2006) showed that for two piers in a tandem arrangement, scour depth reaches its maximum value at a pier spacing of $s = 2D$. Kim et al. (2014) performed numerical simulations to examine scour at two piers for different pier spacing. The results indicated that maximum scour depth was reached when $s = 2.5D$. Wang et al. (2016) found maximum scour depth for $s = 3D$ by conducting long duration tests. In the study of Khaple et al. (2017), pier spacing was within the range of $2D \leq s \leq 12D$ for two piers in a tandem arrangement. The results showed that larger pier spacing led to smaller scour depth discrepancies at the upstream pier. However, maximum scour depth occurred at pier spacing of two and three times

the pier diameter, for which scour depth values were very close. All the above mentioned studies revealed that increasing pier spacing led to increased scour depth. Scour depth reaches its maximum value at a range of $s = 2D - 3D$.

The effect of skew angle on scour depth at pier groups has already been addressed in the literature. However, the number of these reported studies is small, which include those of Laursen and Toch (1956), Hannah (1978), Salim and Jones (1996), Zhao and Sheppard (1999), Sheppard and Renna (2010), Arneson et al. (2012) (HEC-18), Lança et al. (2013), Memar et al. (2018). The study of Laursen and Toch (1956) on scouring at two piers revealed that smaller skew angles cause smaller scour depths at downstream piers. As the skew angle increased, the maximum scour depth at the upstream pier shifted to the downstream pier from $\theta \geq 10°$ (which θ is the skew angle). Hannah (1978) found the maximum scour depth at two tandem piers for skew angles close to $\theta = 45°$. It should be noted that in most past studies, the tests lasted only a few hours without reaching the equilibrium phase. Lança et al. (2013) addressed the effect of test duration, skew angle, pier spacing and number of columns of the pier group on the equilibrium scour depth at pier groups.

Application of collar

Regarding scour reduction techniques at single bridge piers, the use of circular collars has been reported by different researchers (Ettema 1980; Chiew 1992; Kumar, Raju, and Vittal 1999; Zarrati, Gholami, and Mashahir 2004; Zarrati, Nazariha, and Mashahir 2006; Moncada-M et al. 2009; Masjedi, Bejestan, and Esfandi 2010; Tafarojnoruz, Gaudio, and Calomino 2012; Zokaei et al. 2013; Karimaei Tabarestani and Zarrati 2019). For pier groups, Zarrati, Nazariha, and Mashahir (2006) reported the performance of collars for scour reduction around two piers in tandem and side-by-side arrangements. Heidarpour, Afzalimehr, and Izadinia (2010) studied the effect of collars in reducing scour depth at two and three tandem piers.

As can be observed from Figure 1b, a collar is a horizontal disk with a negligible thickness, which is installed adjacent to the base of piers. The collar distributes the approach flow into two zones above and underneath the collar. The collar prevents streambed extraction by downflow and diminishes its strength. Thus, the strength of the horseshoe vortex underneath the collar is also reduced. Previous studies by Zarrati, Nazariha, and Mashahir (2006) and Tafarojnoruz, Gaudio, and Calomino (2012) showed that scouring started downstream of the collar, which subsequently extended toward the collar upstream part around its rim and reached the pier front after a certain time. As a result, the collars postponed scouring in front of the piers. The performance of the collar depends on its width (w_c) and its elevation with respect to the streambed (h_c) (see Figure 1a). Kumar, Raju, and Vittal (1999) proposed an equation to predict the performance of the collar depending on the collar width and elevation. Wider collars close to the streambed can be more efficient than smaller ones (Kumar, Raju, and Vittal 1999). Nevertheless, collars wider than three times the pier diameter appear to be impractical (Zarrati, Nazariha, and Mashahir 2006). Placing the collar at higher elevations above the streambed reduces its performance as more flow can penetrate below the collar (Tanaka and Yano 1967; Zarrati, Gholami, and Mashahir 2004; Moncada-M et al. 2009). However, according to Kumar, Raju, and Vittal (1999), the collar below the streambed may cause maximum scour reduction at piers. Zarrati, Gholami, and Mashahir (2004) showed that at rectangular piers aligned with different skew angles of $0°, 5°$, and $10°$, the optimal collar elevation was on the streambed, where maximum scour reduction occurred. Additionally, lowering the elevation of the collar underneath the streambed increases the scour depth at the pier. Since a part of the sediment above the collar was washed away quickly and was considered as a component of scour depth. In addition, the extension of a scour hole around the pier and at the downstream part of the collar increased. The results obtained by Masjedi, Bejestan, and Esfandi (2010) revealed that at an oblong pier in a 180° flume bend, burying the collar below the streambed approximately 10% of the pier width caused maximum scour reduction. In another study by Moreno, Maia, and Couto (2016) on scour depth at complex bridge piers, the authors found out that minimum scour depth was achieved when the pile cap of the complex pier was partially buried in the streambed. Additionally, results drawn from the above studies clarify that the best elevation of collar resulting in the maximum scour reduction at piers, greatly depends on test conditions, pier shape and alignment. It is important to note that the scouring process at bridge piers continues until the equilibrium scour condition is attained. Accordingly, it is essential for the performance of the collar to be determined in the equilibrium phase.

This study aimed to investigate the performance of collars for scour reduction at two tandem piers aligned with different skew angles of $\theta = 0°, 30°, 60°, 90°$. The few previous studies conducted similar tests for limited times (e.g., 6 hr) and for the skew angle of $\theta = 0°$. In the present study, the tests were carried out for a long time, reaching equilibrium scour conditions after an average of 5 to 8 days. In order to evaluate the performance of collars, the tests were also conducted without collars. In addition, the effect of time was studied on the performance of collars in reducing scour at the piers. Long duration laboratory tests were designed based on the Buckingham theorem. The results are presented in terms of diagnostic analysis and mathematical evaluation for the amount of scour reduction.

Materials and methods

Dimensional analysis

The maximum scour depth d_s around two tandem circular piers with diameter D aligned with skew angle of θ with respect to flow direction, which are preserved with collars at their base in a rectangular flume and with a mobile bed under steady and uniform flow and clear-water conditions over time t, can be described by the following functional relationship (see also Tafarojnoruz, Gaudio, and Calomino 2012):

$$d_s = f\left(\rho, \vartheta, h, B, U, \rho'_s, \ d_{50}, \sigma_g, \ D, t, \theta, \ w_c, h_c, t_c, s, \ U_c\right)$$ (1)

where f = unknown function, ρ = water density, ϑ = water kinematic viscosity, h = approach flow depth, B = flume width, U = mean approach flow velocity, $\rho'_s = \rho_s - \rho$ = buoyant sediment density, ρ_s = sediment density, d_{50} = median sediment size, $\sigma_g = \sqrt{d_{84}/d_{16}}$ is the geometric standard deviation of the sediment size distribution, where d_{84} and d_{16} are the sediment grain sizes at which 84% and 16% of material are finer by weight, h_c = collar elevation with respect to the streambed, w_c = collar width, t_c = collar thickness, s = pier spacing, and U_c = mean threshold velocity. If D, U, and ρ are considered basic variables, by applying the Buckingham theorem to Eq. (1), the dimensionless terms in it can be represented as follows:

$$\frac{d_s}{D} = \varphi\left(\frac{U}{U_c}, \Delta, \frac{UD}{\vartheta}, \frac{s}{D}, \frac{h}{D}, \frac{B}{D}, \frac{w_c}{D}, \frac{h_c}{h}, \frac{t_c}{D}, \frac{Ut}{D}, \frac{D}{d_{50}}, \sigma_g, \theta\right)$$ (2)

In Eq. (2), φ = unknown function, $UD/\vartheta = R_p$ = pier Reynolds number. In Table 1, the test characterizations and nondimensional parameters are summarized. A series and B series tests represent the tests without and with collars, respectively. In order to achieve the equilibrium scour depth

Table 1. Summary of the test characterizations and nondimensional parameters.

Test category	$Q\left(\frac{lit}{s}\right)$	U (m/s)	U/U_C	u_c^* (m)	D (m)	B (m)	d_{50} (m)	h (m)	σ_g	h/D	B/D	D/d_{50}	h_c/h	w_c/D	θ (°)	s/D
A* series	81	0.38	0.95	0.032	0.063	1.3	0.00178	0.165	1.41	2.54	10.32	35.4	–	–	0,30,60,90	3
B** series	77, 81	0.38 0.36	0.95- 0.9	0.032	0.063	1.3	0.00178	0.165	1.41	2.54	10.32	35.4	0, −0.1	2	0,30,60,90	3

Note: Laboratory tests for different skew angle * without collars and ** with collar.

under clear-water conditions, it is essential that the effect of each dimensionless parameter in Eq. (2), be considered before running tests:

The flow intensity was adjusted to a range of $0.9 \leq U/U_c \leq 1$ to attain the equilibrium condition, and $\sigma_g < 1.4$ ensures uniform sediment (Dey, Bose, and Sastry 1995). With nonuniform sediment, the flow causes scattering of the grains and produces an armor layer on the streambed. The coarseness effect on the scour depth, which is caused by the sediment grains size, disappears at $D/d_{50} > 25$ (Melville and Sutherland 1988; Melville 1997). In addition, Tafarojnoruz et al. (2010) suggested a range of $D/d_{50} \approx 25$ to 130, where the influence of the sediment size on scour depth is avoided. Regarding Ettema (1980) for shallow water flows, the interference of the surface roller at the pier ahead and the horseshoe vortex, which turn in opposite directions, influences scour depth around piers; hence, maximum scour depth does not occur. Flow depth was set at $h/D > 2.6$ to be ineffective in the scour process (Melville and Sutherland 1988). The effect of the flume width (blockage effect) on scour depth at bridge piers is omitted if $B/D \geq 10$ (Chiew and Melville 1987). Franzetti, Malavasi, and Piccinin (1994) indicated that if the pier Reynolds number $R_p > 7000$, the viscous effect on the scour process can be overlooked. Relative submerged sediment density $\Delta = \rho'_s/\rho = 1.65$ is constant for gravel and sand (Tafarojnoruz, Gaudio, and Calomino 2012). In this study, all the above mentioned conditions were applied to the tests (see Table 1). Taking all the above into consideration, Eq. (2) becomes:

$$\frac{d_s}{D} = \varphi \left(\frac{U}{U_c}, \frac{s}{D}, \frac{w_c}{D}, \frac{h_c}{h}, \frac{t_c}{D}, \frac{Ut}{D}, \theta \right) \qquad (3)$$

In the present study, almost similar experimental conditions of the study of Khaple et al. (2017) were considered for the tests. Khaple et al. (2017) found out that for two tandem piers, maximum scour depth was attained at pier spacing of two and three times the pier diameter, and that scour depth values of the both pier spacing were almost equal. Therefore, a pier spacing of $s = 3D$ was herein chosen to reach the maximum scour depth at the piers. The piers were equipped with circular PVC transparent collars of width $w_c = 2D$ with a thickness of $t_c = 0.003$ m. The small collar thickness was chosen to not influence the local scouring process. In the equilibrium scour condition, dimensionless time (Ut/D) does not affect the scouring; thus, scour hole dimensions remain constant. Accordingly, Eq. (3) can be simplified by Eq. (4). Figure 1a shows the geometric parameters of tandem piers protected by collars for the skew angle of $\theta = 0°$.

$$\frac{d_{se}}{D} = \varphi \left(\frac{U}{U_c}, \frac{h_c}{h}, \theta \right) \qquad (4)$$

where d_{se} is the equilibrium scour depth.

In the following research, the effect of the collars in reducing the scour depth at two tandem piers aligned with different skew angles of $\theta = 0°, 30°, 60°, 90°$ is examined.

Experimental procedure

The present study was performed in a straight section (with dimensions of 9 m long and 1.3 m width (B)) of a curved flume with PVC sidewalls 0.6 m height in the Laboratory of Hydraulic Constructions (LCH) at the Ecole Polytechnique Fédérale de Lausanne (EPFL) (Figures 2a and 3). To implement the tests, the setup involved placing false floors in the upstream and downstream sections of the straight part of the flume. The interval between the false floors was filled with uniform quartz sand with a diameter of $d_{50} = 0.00178$ m as in the working section, called the recess box that was located 4 m from the flume entrance, with dimensions of 5 m long, 1.3 m width, and 0.25 m high. To sustain the same roughness throughout the entire flume, the desired sediments were glued to the false floors. The cylindrical piers with a diameter of 0.063 m were simulated using transparent PVC pipe located 7 m from the flume entrance to ensure a fully developed flow in the test region. Prior to conducting each test, the streambed was compacted and carefully leveled by using a small flat wooden plate. The area surrounding the piers was covered by a thin, transparent plate to avoid uncontrolled scour depth at the beginning of the test. Afterwards, a small discharge (4 l/s) was set to feed the flume without disturbing the streambed. Water entered the flume inlet basin through a constant discharge basin. A metal net with an attached filter sponge was installed in the inlet basin to ensure a uniform flow distribution. Additionally, an XPS (extruded polystyrene) diffuser plate was floated on the water surface close to the entrance of the flume to damp the flow fluctuations. The discharge was supplied by an automatically operated pump and was measured with a discharge meter. A flap gate was located at the downstream end of the flume before the outlet basin, allowing the flow depth to be regulated (Figures 2b and 3). The discharge was gradually increased until the desired mean flow velocity was obtained in the flume. Immediately, the transparent plate was removed, and the test started. A digital point gauge with an accuracy of 0.1 mm was utilized to measure the flow depth. A constant approach flow depth equal to 0.165 m was adjusted in all tests. Time evolution of the scour depth was recorded by ruler paper attached to the transparent piers by means of a periscope located inside the model piers. After the tests were stopped, once almost all the water was drained slowly from the flume in some of the tests, the topography of the eroded streambed was digitized by a three-dimensional (3D) laser Baumer, OADM 13I7480/ S35A (Figure 2c). Instruments were installed on the moving carriage, positioned at the upper part of the flume as shown in the plan view of the experimental setup in Figures 2d and 3. As already mentioned in the previous section, the experiments had to be designed such that the impact of sediment size, blockage, viscous and flow shallowness on the evolution of scour depth could be neglected. All tests were conducted near the threshold of sediment motion. The values of mean threshold velocity (U_c) and shear critical velocity (u_c^*) were initially estimated through the Shields diagram and empirical equations introduced by Melville and Sutherland (1988), Sheppard, Melville, and Demir (2014) and Shamov (1952)
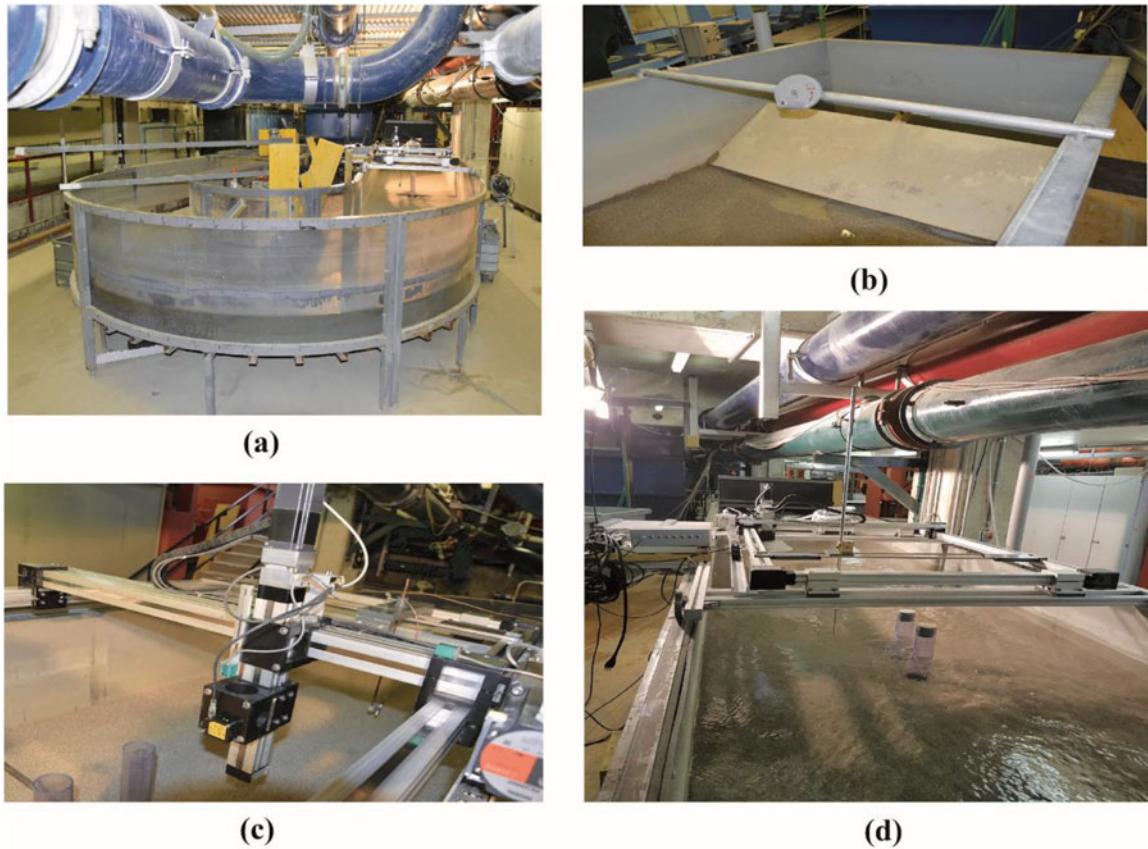
Figure 2. Front view of the flume (a), downstream flap gate (b), 3D laser Baumer, OADM 13I7480/S35A (c), moving carriage (d).
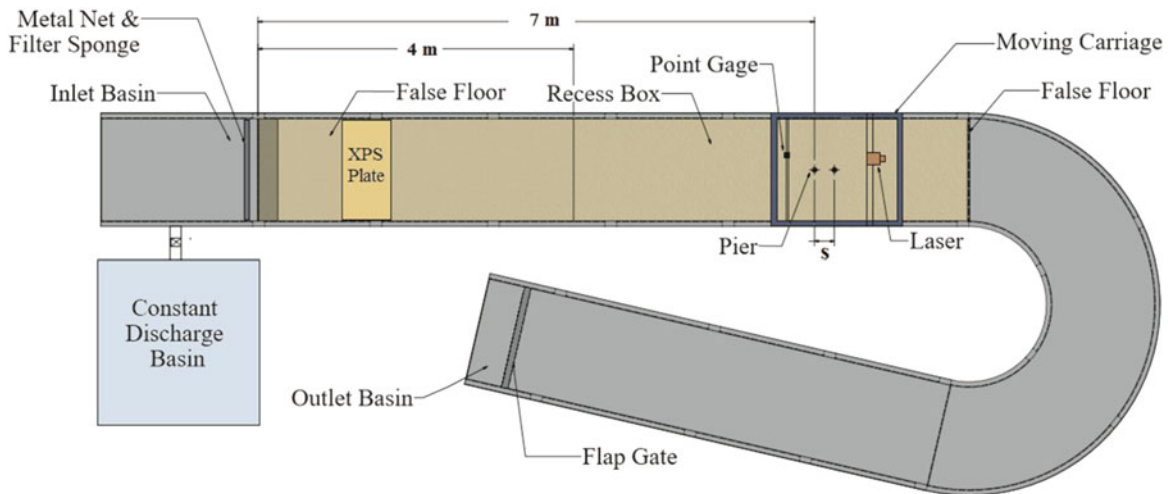

Figure 3. Plan view of the experimental setup.

(which is mentioned in the study of Dey (2014)). Afterwards, some tests were performed in the absence of the piers, and the mean threshold velocity was specified. The results were in good agreement with the equation of Shamov (1952) (which is mentioned in the study of Dey (2014)) (Eq. 5).

$$\frac{U_c}{\sqrt{g.d_{50}}} = 1.47\left(\frac{h}{d_{50}}\right)^{\left(\frac{1}{6}\right)} \tag{5}$$

where g is the gravitational acceleration.

Duration of the tests

To achieve the equilibrium scour condition, sufficient test time is required for the scouring rate to become negligible. Benchmarks have been appointed for ending the test by different researchers. According to Franzetti, Malavasi, and Piccinin (1994), equilibrium conditions at bridge piers occur when $(Ut/D > 2*10^6)$, where Ut/D is dimensionless time and D is the pier diameter. Melville and Chiew (1999) introduced the equilibrium time of scour as a condition in which the scouring rate variations were less than 5% of the pier

diameter during 24 hr $(\Delta d_s \leq 0.05D)$. A more cautious criterion is suggested by Grimaldi (2005), which is described as $\Delta d_s \leq 0.05D/3$. The predictors of time were recommended to approximate the finite equilibrium time of scour at bridge piers by Melville and Chiew (1999) and Kothyari, Hager, and Oliveto (2007). Nevertheless, Oliveto and Hager (2002, 2005) highlighted that the scouring process may continue even after scour geometry seems to reach the equilibrium state. Lança, Fael, and Cardoso (2010) suggested calculating the equilibrium scour depth at infinite time $(t = \infty)$ by adjusting the polynomial function to the recorded time evolution of the scour depth.

In this study, all tests were performed for a long time, achieving equilibrium scour conditions. The equilibrium time of the scour, t_e, was estimated by using the predictor of Melville and Chiew (1999), taking into consideration the effective width of an equivalent full depth pier (D^*) provided by the Federal Highway Administration, HEC-18 (Arneson et al. 2012), to account for the pier's interaction effect, as follows:

$$t_e(\text{days}) = 48.26 \frac{D^*}{U} \left(\frac{U}{U_C} - 0.4 \right) \text{ for } \frac{h}{D^*} > 6 \qquad (6)$$

$$t_e(\text{days}) = 30.89 \frac{D^*}{U} \left(\frac{U}{U_C} - 0.4 \right) \left(\frac{h}{D^*} \right)^{0.25} \text{ for } \frac{h}{D^*} \leq 6 \qquad (7)$$

$$D^* = D_{\text{proj}} * K_{\text{sp}} * K_m \qquad (8)$$

where D_{proj} is the sum of the nonoverlapping projected widths of piers, K_{sp} is the pier spacing coefficient and K_m is the number of aligned rows coefficient. The tests were stopped per the criterion of Melville and Chiew (1999). However, by substituting the D^* with D in Eq. (7), it was found that the calculated equilibrium time was in better agreement with the scour depth recorded at the end of the test. Thus, by using D^* instead of D in Eq. (7), the results are closer to the equilibrium scour depth measured at the end of the tests, d_{se}. According to Chabert and Engeldinger (1956) and Ettema (1980), it can be assumed that the equilibrium scour condition is achieved asymptotically. Thus, the measured equilibrium scour depth at the end of the test, d_{se}, can then be extrapolated to the infinite time $(t = \infty)$ by adjusting a six-parameter polynomial function suggested by Lança, Fael, and Cardoso (2010) to the time evolution of the scour depth. Additionally, the extrapolated scour depth to

infinite time $d_{s(\text{ext})}$ (final state), which is correlated to each individual pier, is specified (Table 2).

$$d_s = P_1 \left(1 - \frac{1}{1 + P_1 P_2 t} \right) + P_3 \left(1 - \frac{1}{1 + P_3 P_4 t} \right) + P_5 \left(1 - \frac{1}{1 + P_5 P_6 t} \right) \qquad (9)$$

where d_s is the maximum scour depth at a time t, the parameters P were obtained via regression analysis. At the infinite time $(t = \infty)$ the value of the scour depth is $d_s = P_1 + P_3 + P_5$.

Results and discussion

The performance of collars was investigated for scour reduction at two tandem piers aligned with different skew angles of $= 0°, 30°, 60°, 90°$. For this purpose, two series of long-lasting tests were conducted: without collars (series A) and with collars (series B). Figure 4 schematically depicts the alignment of the tandem piers with the four different skew angles for both A series without collars and B series with collars (see Table 2) in the laboratory tests.

The performance of collars for the skew angle of $\theta=0°$

In order to achieve the maximum scour reduction at the piers, the proper collar elevation with respect to the streambed (h_c) needs to be considered. To do this, the collars were placed on the streambed, $h_c = 0$, and below the streambed at $h_c = -0.1h$, where h is the approach flow depth. The tests were performed with flow intensities of $U/U_c = 0.9, 0.95$.

It should be clarified that the initial collars had a width $w_c = 3D$, where D is the pier diameter, and were tested at a flow intensity of 0.9. It was observed that no scour occurred in front of the piers after almost 10 days. The scouring started at the rear of the downstream collar and then extended upstream around the rims of the collars but did not reach the piers front. Therefore, in an attempt to carry out better observations of the scouring evolution around the piers, smaller collars with a width $w_c = 2D$ were chosen to evaluate the performance of collars at different skew angles.

Figure 5 shows a comparison of the evolution of scour depth in front of the upstream pier for different collar elevations. The results indicated that the best location for collars was on the streambed, where the maximum scour reduction

Table 2. Equilibrium scour depth, d_{se}, equilibrium time of the scour t_e, extrapolated values of the scour depth at an infinite time $d_{s(\text{ext})}$, scour reduction R, for two tandem piers aligned with different skew angles θ, with and without collars of width $w_c = 2D$.

Test	collar	θ (°)	U/U_c	d_{se1} (m)	d_{se2} (m)	t_e (hr)	$d_{s(\text{ext})1}$ (m)	$d_{s(\text{ext})2}$ (m)	R_1 (%)	R_2 (%)	Δd_{s1} (%)	Δd_{s2} (%)
A1	without	0	0.95	0.129	0.096	120	0.145	0.106	_	_	12.403	10.417
B1	with	0	0.95	0.106	0.065	144	0.1247	0.081	17.83	32.29	17.642	24.615
A2	without	30	0.95	0.136	0.139	130	0.149	0.163	_	_	9.559	17.266
B2	with	30	0.95	0.113	0.134	168	0.1251	0.1671	16.3	2.9	10.708	24.701
A3	without	60	0.95	0.143	0.157	144	0.156	0.183	_	_	9.091	16.561
B3	with	60	0.95	0.131	0.155	192	0.147	0.206	8.39	1.91	12.214	32.903
A4	without	90	0.95	0.142	0.141	120	0.154	0.153	_	_	8.451	8.511
B4	with	90	0.95	0.123	0.121	168	0.142	0.138	13.38	14.18	15.447	14.050

Note: $_1$ and $_2$ are related to the upstream and downstream piers respectively.
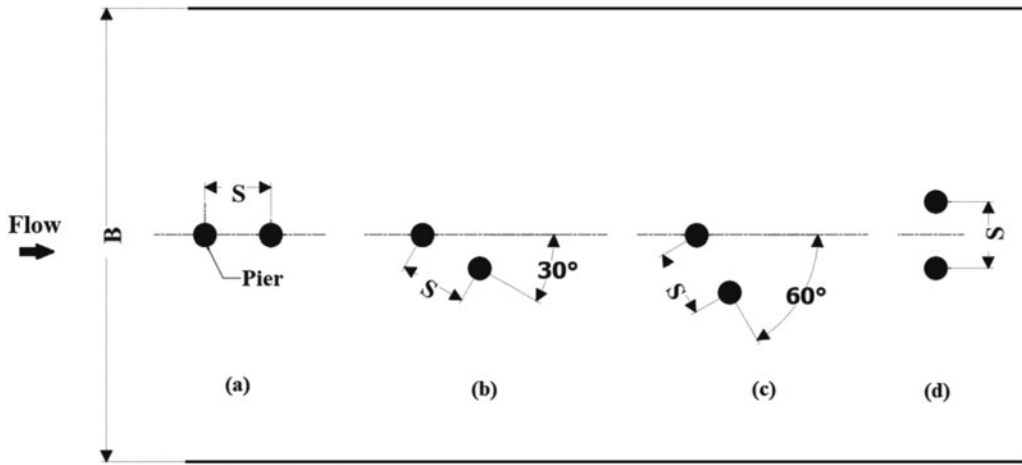
Figure 4. Test configurations for different skew angles: (a) $\theta = 0°$; (b) $\theta = 30°$; (c) $\theta = 60°$; (d) $\theta = 90°$.
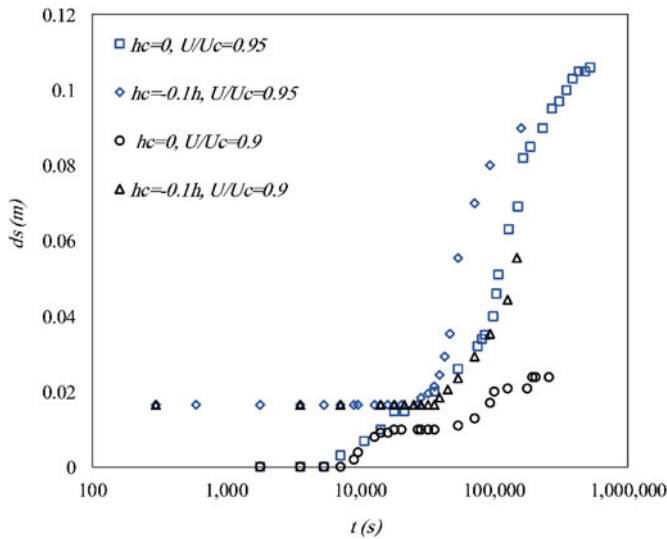

Figure 5. Evolution of the scour depth around the upstream pier, d_s, at collar elevations of $h_c = 0$ and $h_c = -0.1h$, for $\theta = 0°$ with different flow intensities (U/U_c), on a logarithmic scale (h is the approach flow depth).

Figure 6. Tandem piers protected by collars aligned with the skew angle of $\theta = 0°$.

was reached. When $h_c = -0.1h$, sediments on the collars were scoured nearly 5 min after the test began. The results revealed that, by shifting the collars under the bed, a larger scour depth occurred although the scouring reached the pier front later than the situation when the collars were placed on the bed. The portion of the sediments on the collars was accounted for as part of the scour depth. Additionally, the extension of the scour hole around the piers increased. Therefore, the rest of the tests were performed with the collars being located on the streambed. Furthermore, the flow intensity had a significant influence on the scour depth at the piers. Indeed, increasing the flow intensity from 0.9 to 0.95 increased the scour depth in front of the piers by about 4.6 times and the equilibrium time of the scour (t_e) was almost doubled. Karimaei Tabarestani and Zarrati (2019) also declared that the flow intensity was a major parameter influencing the performance of collars for scour reduction at piers.

It is noteworthy that the previous studies by Tanaka and Yano (1967) and Zarrati, Gholami, and Mashahir (2004)
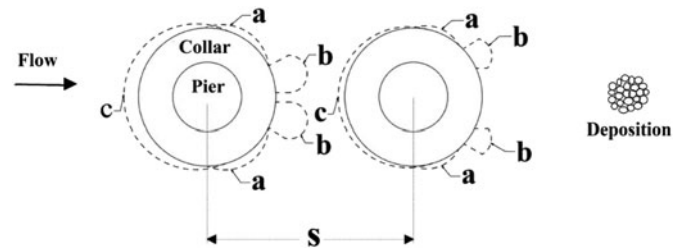
showed that by increasing the collar elevation above the streambed, more flow could penetrate below the collar; therefore, the performance of the collar diminished. Given this result, the performance of collars for scour reduction when placed above the streambed is not investigated in this study.

As can be observed from Figure 6, for the skew angle of $\theta = 0°$ and $h_c = 0$, $U/U_c = 0.95$ at the beginning of the test, scouring initiates downstream from the rims of the collars (region a). A possible interpretation is that the interaction of approach flow with the piers creates boundary layer flows along the upstream pier perimeter. Separation of the boundary layer flows from the sides of the piers causes the maximum pressure gradient and the corresponding maximum bed shear stress, taking in to account the study of Guo et al. (2012). Sediments were swept up owing to the action of wake vortices at the rear of the collars (region b); subsequently, two holes were developed after almost 20 min (region b). The holes enlarged and expanded upstream (region c). The scour reached the upstream pier front after 120 min. For the downstream pier, scouring reached the pier front later at 180 min. Due to the sheltering effect from the upstream pier, the approach velocity toward the downstream pier is reduced and thus the scouring rate decreases. Additionally, at the rear of its collar, the holes became wider and deeper, developing downstream of the flume and forming sediment deposition in the lower part of the wake vortices, where the large vortices broke into small eddies by viscosity (downstream section of the region b of the downstream pier) (see also Guo et al. 2012). The equilibrium

scour around tandem piers protected by collars for $\theta = 0°$ is illustrated with contour lines in Figure 7.

In order to evaluate the performance of the collars for scour reduction in front of the piers, the dimensionless evolution of scour depths with and without the collars ($w_c = 2D$, $h_c = 0$) for different skew angles were compared, as in Figure 8, by using the dimensionless time term suggested by Yilmaz, Yanmaz, and Koken (2017) and by
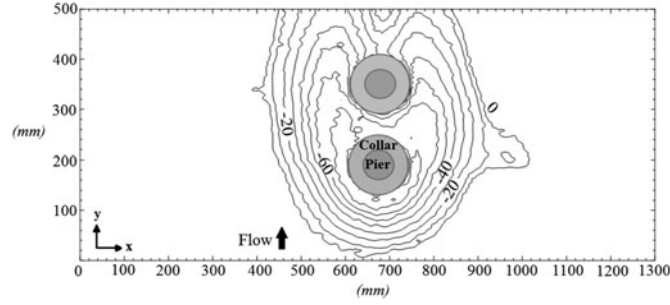
Figure 7. Contour lines of the equilibrium scour depth around tandem piers protected by collars for $\theta = 0°$.

substituting the pier diameter (D) by D^* as follows (see also Table 2):

$$T_s = \frac{t d_{50}(\Delta g d_{50})^{0.5}}{D^{*2}} \qquad (10)$$

$$S = \frac{d_s}{D^*} \qquad (11)$$

where S = dimensionless scour depth, d_s = scour depth, T_s = dimensionless time, t = time, $\Delta = \rho'_s/\rho$, ρ = water density, $\rho'_s = \rho_s - \rho$ = buoyant sediment density, ρ_s = sediment density, d_{50} = median sediment size and D^* = the effective width of an equivalent full depth pier suggested by the Federal Highway Administration (FHWA) (HEC-18) (Arneson et al. 2012). The parameters P_u and P_d represent the upstream and downstream piers, respectively.

For all the skew angles, the collars postponed the scouring evolution in front of the piers and decreased the scouring rate compared to that for the tests without the collars. This conclusion was also reported by Zarrati, Nazariha, and Mashahir (2006), Heidarpour, Afzalimehr, and Izadinia
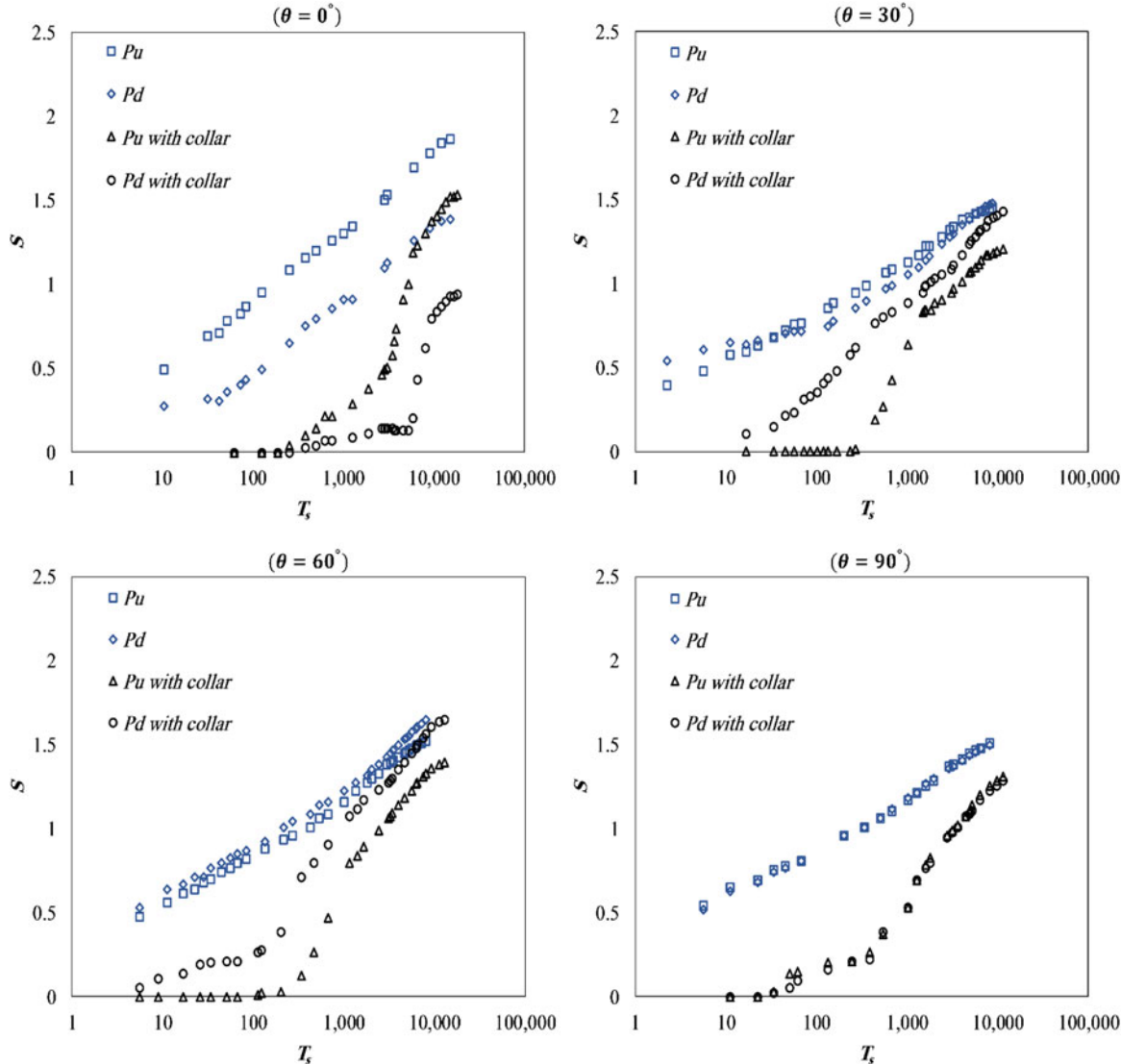
Figure 8. Dimensionless evolution of the scour depth in front of two tandem piers aligned with different skew angles with and without collars by using dimensionless time term of Yilmaz, Yanmaz, and Koken (2017), on a logarithmic scale.
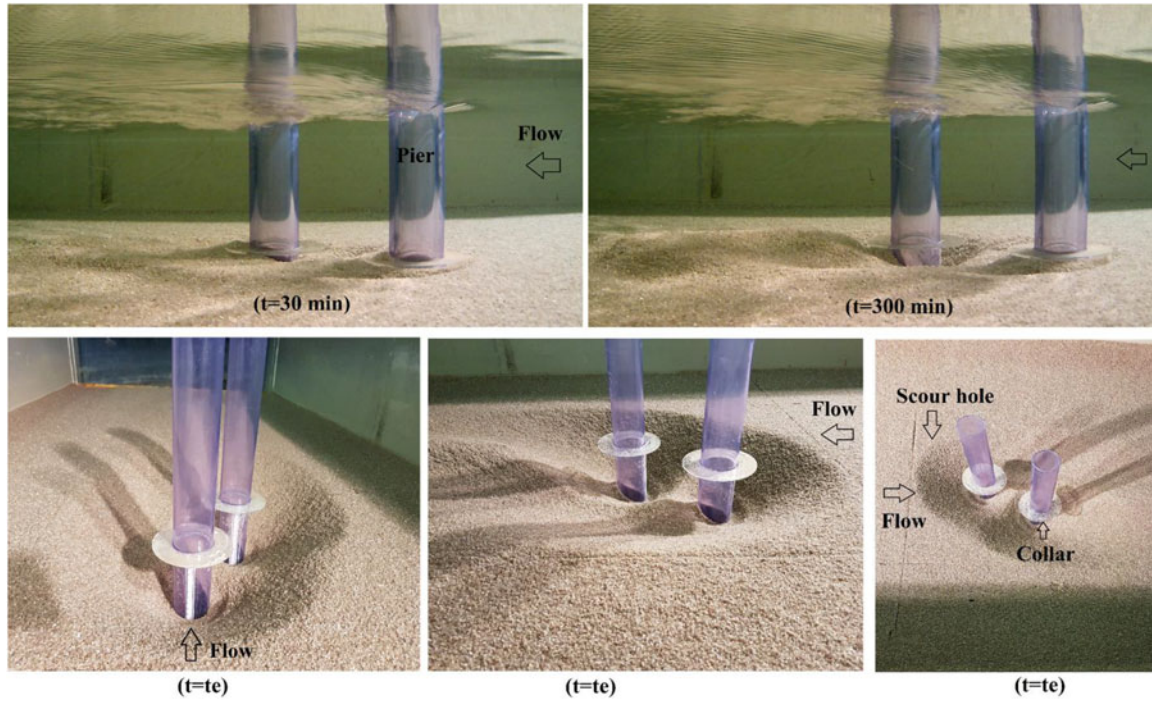
Figure 9. Eroded streambed at tandem piers aligned with the skew angle of $\theta = 30°$ for different times and at the equilibrium time $(t = t_e)$.
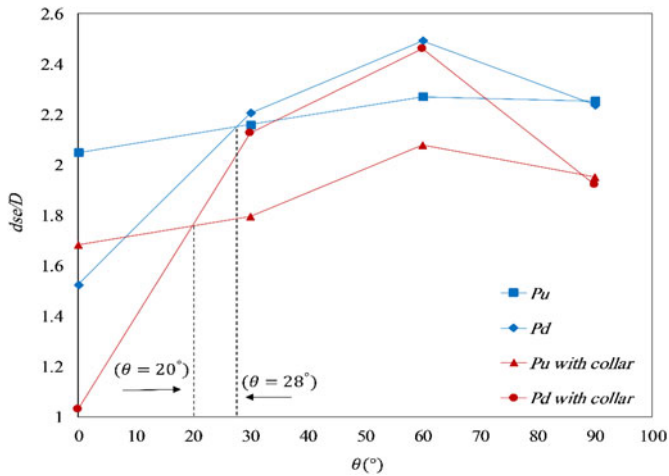

Figure 10. Effect of the skew angle on equilibrium scour depth d_{se} at tandem piers with and without collars.

(2010), Tafarojnoruz, Gaudio, and Calomino (2012) and Karimaei Tabarestani and Zarrati (2019).

The performance of collars for the skew angles of $\theta = 30°, 60°, 90°$

For the skew angle of $\theta = 30°$ and $h_c = 0$ (test B2, Table 2), scouring initiated at an interval between piers; thus, a hole was produced and expanded toward the piers and downstream section. Instantaneously, the downstream rims of collars were scoured, and two small holes were generated at the rear of the collars and extended upstream. The scouring rate at the downstream pier was higher than that at the upstream pier. Scour reached the pier front after 210 min and 5 min of the upstream and downstream piers, respectively. By

Table 3. The values of dimensionless scour depth (d_s/D) for different skew angles and Percentages of discrepancy (Δd_s) between the results of the present study and the study of Hannah (1978).

	Upstream pier				Downstream pier			
$\theta(°)$	0	30	60	90	0	30	60	90
Present study	2.05	2.15	2.27	2.25	1.52	2.21	2.49	2.24
Hannah (1978)	2.06	2.09	2.092	2.03	1.77	2.06	2.2	2.07
(Δd_s)	0.48	2.79	7.84	9.77	16.44	6.78	11.64	7.59

increasing the skew angle, the downstream pier is exposed to the approach flow entirely. Likewise, the sheltering effect from the upstream pier is reduced, and the interference of vortices enhances the scouring rate around the downstream pier. The equilibrium scour depth at the upstream pier is approximately 86% of the scour depth around the downstream pier (Figure 8, $\theta = 30°$). Figure 9 shows the eroded streambed at different times and at the equilibrium state $(t = t_e)$ for the skew angle of $\theta = 30°$.

The evolution of the scour depth for the skew angle of $\theta = 60°$ (test B3) was similar to that for $\theta = 30°$. Scour achieved the upstream and downstream piers face after 100 min and 5 min, respectively. The equilibrium scour depth at the upstream pier is approximately 86% of that at the downstream pier (Figure 8). For $\theta = 90°$ (test B4), similar to the other cases, scouring originated at the downstream rims of the collars, and two scour holes were generated, expanding to their upstream and downstream sections. Scour reached the pier fronts after 30 min. The scouring rate increased significantly as soon as all the sediments were washed away around the piers after almost 340 min ($T_s > 380$) (Figure 8). The scour depth at the both piers is almost identical.

The value of scour depth reduction (R) in front of the piers is given in Table 2 and is calculated using Eq. (12).

Table 4. The values of percent scour reduction R at different times.

	R_1 (%)					R_2 (%)				
θ (°)	$t = 5$(hr)	$t = 21$(hr)	$t = 40$(hr)	$t = 72$(hr)	$t = t_e$	$t = 5$(hr)	$t = 21$(hr)	$t = 40$(hr)	$t = 72$(hr)	$t = t_e$
0	82.35	68.63	39.82	23.58	17.83	91.23	86.67	89.15	41.30	32.29
30	94.62	30.00	29.26	23.66	16.30	26.19	14.53	15.25	10.77	2.90
60	86.96	31.40	24.22	18.25	8.39	33.00	12.50	10.61	8.97	1.91
90	76.84	41.70	29.69	23.53	13.38	78.95	42.60	29.92	23.70	14.18

$$R(\%) = \frac{d_{se0} - d_{se}}{d_{se0}} * 100 \qquad (12)$$

where the subscript 0 represents the test without the collar. Increasing the skew angle decreased the performance of the collars at the both piers. The minimum and maximum scour depth reduction in the equilibrium state was obtained for the skew angles of $\theta = 60°$ and $\theta = 0°$, respectively (see Table 2). The parameters d_{se1} and d_{se2} represented the equilibrium scour depth in front of the upstream and downstream piers, respectively. The results were then extrapolated to an infinite time ($t = \infty$) by utilizing the Eq. 9. The extrapolated scour depths in front of the piers were shown by $d_{s(ext)}$. In addition, in Table 2, the quantities of percent deviation (Δd_s) of the equilibrium scour depth (recorded at the end of the tests), d_{se}, with the extrapolated ones, $d_{s(ext)}$, revealed that in most of our tests, almost 90% of the extrapolated scour depth occurred. Thus, the results were close to scour depths at infinite time.

Figure 10 highlights the influence of the skew angle on the local scour depth at the tandem piers with and without the collars. The vertical axis represents the dimensionless equilibrium scour depth (d_{se}/D), in which D is the pier diameter. With increasing the skew angle, the variations of the scour depths were low for the upstream pier whereas they were significant for the downstream pier. The maximum and minimum equilibrium scour depths in front of both the piers with and without the collars were obtained for the skew angles of $\theta = 60°$ and $\theta = 0°$, respectively. The analysis of the results shows that the maximum equilibrium scour depth from the upstream pier is shifted to the downstream pier from $\theta \geq 20°$ $\theta \geq 28°$ for tests with and without collars, respectively. A comparison between the results obtained from the present study (for the tests without the collars) and those obtained by Hannah (1978) is shown in Table 3. Increasing the skew angle increased the scour depth in both the studies. The difference between the scour depths of the two studies may be associated with the short duration of the tests (7 hr) in the study conducted by Hannah (1978). Differences of pier spacing can be another reason, since pier spacing was five times the pier diameter in the Hannah study (1978).

Effect of time on collar performance

As stated earlier, local scouring at bridge piers is continuous until the equilibrium scour phase is obtained. Accordingly, the actual collar performance needs to be presented in the equilibrium time. From Table 2, it becomes clear that the equilibrium time of the scour (t_e) increased systematically with θ and reached its maximum value at $\theta = 60°$, and then
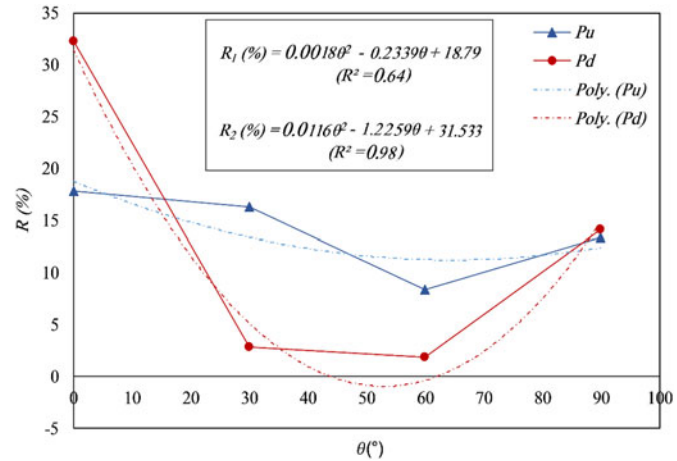
Figure 11. Scour reduction values for different skew angles.

decreased for $\theta = 90°$. It was observed that the tests with the collars needed a longer time to reach the equilibrium state in comparison with the tests without the collars (almost 24 hr for $\theta = 0°$, 38 hr for $\theta = 30°$, 48 hr for $\theta = 60°$ and 72 hr for $\theta = 90°$).

Table 4 summarizes the scour reduction values, R_1 and R_2, at the upstream and downstream piers, respectively, obtained at $t = 5, 21, 40, 72$ hr and $t = t_e$. The results revealed that the performance of the collars was reduced over the time t, since as the scour hole around the piers and collars developed, the scouring rate increased. The scour reduction (R) reached greater values during the first hours of the tests (see $t = 5$ hr) and reached its minimum value in the equilibrium time, for all the skew angles. The performance of the collars was insignificant for $\theta = 60°$. These outcomes are in agreement with those found in the previous studies. In the study of Moncada-M et al. (2009), the collar performance obtained was 100%, since the tests were conducted for short durations (6 hr). While, Tafarojnoruz, Gaudio, and Calomino (2012) observed 28% scour reduction at a single pier protected by the collar in the equilibrium time. The scour reduction values for the different skew angles are illustrated in Figure 11.

Conclusions

In this study, the performance of the collars was assessed for scour reduction in front of the two tandem piers aligned with the skew angles of $\theta = 0°, 30°, 60°, 90°$. The results revealed that the equilibrium scour depth in front of the piers with and without the collars increased systematically with increasing the skew angle (θ) and reached the maximum value at $\theta = 60°$, and then decreased. Consequently,

increasing the skew angle decreased the performance of the collars. The maximum and minimum equilibrium scour depths in front of the two tandem piers without and with the collars were obtained for the skew angles of $\theta = 60°$ and $\theta = 0°$ for the both piers, respectively. In addition, by increasing the skew angle, the equilibrium time of the scour t_e increased. Moreover, the performance of the collars for scour reduction decreased over the time t until the equilibrium scour phase was obtained.

For the two tandem piers protected by the collars, by placing the collars under the streambed, the scour reached the piers front later than the situation when the collars were on the streambed; however, the scour depth increased and the scour hole extension was greater. According to the analysis of the results, the maximum scour depth from the upstream pier shifted to the downstream pier for $\theta \geq 20°$ and $\theta \geq 28°$ for two tandem piers aligned with different skew angles with and without the collars, respectively.

Notations

The following symbols are used in this paper:

B	flume width
D	pier diameter
D^*	effective width of an equivalent full depth pier
D_{proj}	sum of the nonoverlapping pier widths projected on a plane normal to the approach flow direction
d_s	maximum scour depth
d_{se}	equilibrium scour depth
$d_{s(ext)}$	extrapolated scour depth to the infinite time
d_{50}	median sediment size
f	unknown function
g	gravitational acceleration
h	approach flow depth
h_c	collar elevation with respect to the streambed
K_m	number of aligned rows coefficient
K_{sp}	pier spacing coefficient
R	scour depth reduction
$R_p = UD/\vartheta$	pier Reynolds number
S	dimensionless scour depth
s	pier spacing
t_c	collar thickness
U	mean approach flow velocity
U_c	mean threshold velocity
u_c^*	shear critical velocity
T_s	dimensionless time
t	time
t_e	equilibrium time of scour
$\Delta = \rho_s'/\rho$	relative submerged sediment density
θ	skew angle with respect to flow direction
ϑ	water kinematic viscosity
ρ	water density
ρ_s	sediment density
ρ_s'	buoyant sediment density
σ_g	geometric standard deviation of sediment size distribution; and
φ	unknown function.

ORCID

Sargol Memar http://orcid.org/0000-0003-2980-5067
Mohammad Zounemat-Kermani http://orcid.org/0000-0002-1421-8671
Aliasghar Beheshti http://orcid.org/0000-0002-0951-9568
Majid Rahimpour http://orcid.org/0000-0001-6165-994X
Giovanni De Cesare http://orcid.org/0000-0002-1117-3180
Anton J. Schleiss http://orcid.org/0000-0003-1559-5740

References

Amini, A., and T. A. Mohammad. 2017. Local Scour Prediction around Piers with Complex Geometry. *Marine Georesources and Geotechnology* 35 (6): 857–864. doi:10.1080/1064119X.2016.1256923.

Amini, A., and N. Solaimani. 2018. The Effects of Uniform and Nonuniform Pile Spacing Variations on Local Scour at Pile Groups. *Marine Georesources and Geotechnology* 36 (7): 861–866. doi:10.1080/1064119X.2017.1392658.

Arneson, L. A., L. W. Zevenbergen, P. F. Lagasse, and P. E. Clopper. 2012. *Evaluating Scour at Bridges*. 5th ed. FHWA Publication Number: HIF- 12–003. USA: U.S. Department of Transportation. Federal Highway Administration.

Ataie-Ashtiani, B., and A. A. Beheshti. 2006. Experimental Investigation of Clear-Water Local Scour at Pile Groups. *Journal of Hydraulic Engineering* 132 (10): 1100–1104. doi:10.1061/(ASCE)0733-9429(2006)132:10(1100).

Beg, M. 2004. Mutual interference of bridge piers on local scour. In Proceedings 2nd International Conference on Scour and Erosion (ICSE-2). November 14–17, Singapore.

Beg, M., and S. Beg. 2015. Scour Hole Characteristics of Two Unequal Size Bridge Piers in Tandem Arrangement. *ISH Journal of Hydraulic Engineering* 21 (1): 85–96. doi:10.1080/09715010.2014.963176.

Chabert, J., and P. Engeldinger. 1956. *Study of Scour around Bridge Piers*. Report Prepared for the Laboratoire National d'Hydraulique.

Chiew, Y. M. 1992. Scour Protection at Bridge Piers. *Journal of Hydraulic Engineering* 118 (9): 1260–1269. doi:10.1061/(ASCE)0733-9429(1992)118:9(1260).

Chiew, Y. M., and B. W. Melville. 1987. Local Scour around Bridge Piers. *Journal of Hydraulic Research* 25 (1): 15–26. doi:10.1080/00221688709499285.

Dey, S. 2014. *Fluvial Hydrodynamics*. Berlin: Springer.

Dey, S., S. K. Bose, and G. L. N. Sastry. 1995. Clear Water Scour at Circular Piers: A Model. *Journal of Hydraulic Engineering* 121 (12): 869–876. doi:10.1061/(ASCE)0733-9429(1995)121:12(869).

Ettema, R. 1980. *Scour at Bridge Piers*. Report. No. 216. Auckland, New Zealand: University of Auckland.

Franzetti, S., S. Malavasi, and C. Piccinin. 1994. Sull'erosione alla base pile di ponte in acquechiare. *Proceedings of the 24th conference of hydraulics and hydraulic constructions*, Napoli, Italy (in Italian).

Grimaldi, C. 2005. Non-Conventional Countermeasures against Local Scouring at Bridge Piers. PhD diss., University of Calabria.

Guo, J., O. Suaznabar, H. Shan, and J. Shen. 2012. *Pier Scour in Clear-Water Conditions with Non-Uniform Bed Materials* (Report No. FHWA-HRT-12-022). Turner-Fairbank Highway Research Center.

Hamidi, A., and S. M. Siadatmousavi. 2017. Numerical Simulation of Scour and Flow Field for Different Arrangements of Two Piers Using SSIIM Model. *Ain Shams Engineering Journal* 9 (4): 2415–2426. doi:10.1016/j.asej.2017.03.012.

Hannah, C. R. 1978. *Scour at Pile Groups*. Report No. 78-3. New Zealand, Canterbury: Canterbury University.

Heidarpour, M., H. Afzalimehr, and E. Izadinia. 2010. Reduction of Local Scour around Bridge Pier Groups Using Collars. *International*

Journal of Sediment Research 25 (4): 411–422. doi:10.1016/S1001-6279(11)60008-5.

Karimaei Tabarestani, M., and A. R. Zarrati. 2019. Local scour depth at a bridge pier protected by a collar in steady and unsteady flow. Proceedings of the Institution of Civil Engineers-Water Management. Thomas Telford Ltd, London, United Kingdom. doi:10.1680/jwama.18.00061.

Keshavarzi, A., C. K. Shrestha, B. W. Melville, H. Khabbaz, M. Ranjbar-Zahedani, and J. Ball. 2018. Estimation of Maximum Scour Depths at Upstream of Front and Rear Piers for Two in-Line Circular Columns. *Environmental Fluid Mechanics* 18 (2): 537–550. doi:10.1007/s10652-017-9572-6.

Khaple, S., P. R. Hanmaiahgari, R. Gaudio, and S. Dey. 2017. Interference of an Upstream Pier on Local Scour at Downstream Piers. *Acta Geophysica* 65 (1): 29–46. doi:10.1007/s11600-017-0004-2.

Kim, H. S., M. Nabi, I. Kimura, and Y. Shimizu. 2014. Numerical Investigation of Local Scour at Two Adjacent Cylinders. *Advances in Water Resources* 70: 131–147. doi:10.1016/j.advwatres.2014.04.018.

Kothyari, U. C., W. H. Hager, and G. Oliveto. 2007. Generalized Approach for Clear-Water Scour at Bridge Foundation Elements. *Journal of Hydraulic Engineering* 133 (11): 1229–1240. doi:10.1061/(ASCE)0733-9429(2007)133:11(1229).

Kumar, V., K. G. R. Raju, and N. Vittal. 1999. Reduction of Local Scour around Bridge Piers Using Slots and Collars. *Journal of Hydraulic Engineering* 125 (12): 1302–1305. doi:10.1061/(ASCE)0733-9429(1999)125:12(1302).

Lança, R., C. Fael, and A. Cardoso. 2010. Assessing equilibrium clear water scour around single cylindrical piers. Proceedings of the International Conference on Fluvial Hydraulic (River Flow), Braunschweig, Germany, September 8–10.

Lança, R., C. Fael, R. Maia, J. P. Pêgo, and A. H. Cardoso. 2013. Clear-Water Scour at Pile Groups. *Journal of Hydraulic Engineering* 139 (10): 1089–1098. doi:10.1061/(ASCE)HY.1943-7900.0000770.

Laursen, E. M., and A. Toch. 1956. *Scour around Bridge Piers and Abutments.* Bulletin No.4, Ames, IA: Iowa Highways Research Board.

Liang, F., C. Wang, and X. Yu. 2018. Widths, Types, and Configurations: Influences on Scour Behaviors of Bridge Foundations in Non-Cohesive Soils. *Marine Georesources and Geotechnology* 37 (5):578–588.

Liang, F., C. Wang, M. Huang, and Y. Wang. 2017. Experimental Observations and Evaluations of Formulae for Local Scour at Pile Groups in Steady Currents. *Marine Georesources and Geotechnology* 35 (2): 245–255. doi:10.1080/1064119X.2016.1147510.

Masjedi, A., M. S. Bejestan, and A. Esfandi. 2010. Reduction of Local Scour at a Bridge Pier Fitted with a Collar in a 180 Degree Flume Bend (Case Study: Oblong Pier). *Journal of Hydrodynamics* 22 (S1): 646–650. doi:10.1016/S1001-6058(10)60012-1.

Melville, B. W. 1997. Pier and Abutment Scour: integrated Approach. *Journal of Hydraulic Engineering* 123 (2): 125–136. doi:10.1061/(ASCE)0733-9429(1997)123:2(125).

Melville, B. W., and A. J. Sutherland. 1988. Design Method for Local Scour at Bridge Piers. *Journal of Hydraulic Engineering* 114 (10): 1210–1226. doi:10.1061/(ASCE)0733-9429(1988)114:10(1210).

Memar, S., M. Zounemat-Kermani, A. A. Beheshti, G. De Cesare, and A. J. Schleiss. 2018. Investigation of local scour around tandem piers for different skew-angles. International conference on fluvial hydraulics (River flow), Lyon-Villerurbanne, France, September 5–8.

Moncada-M, A. T., J. Aguirre-Pe, J. C. Bolivar, and E. J. Flores. 2009. Scour Protection of Circular Bridge Piers with Collars and Slots. *Journal of Hydraulic Research* 47 (1): 119–126. doi:10.3826/jhr.2009.3244.

Moreno, M., R. Maia, and L. Couto. 2016. Effects of Relative Column Width and Pile-Cap Elevation on Local Scour Depth around Complex Piers. *Journal of Hydraulic Engineering* 142 (2): 04015051. doi:10.1061/(ASCE)HY.1943-7900.0001080.

Oliveto, G., and W. H. Hager. 2002. Temporal Evolution of Clear-Water Pier and Abutment Scour. *Journal of Hydraulic Engineering* 128 (9): 811–820. doi:10.1061/(ASCE)0733-9429(2002)128:9(811).

Oliveto, G., and W. H. Hager. 2005. Further Results to Time-Dependent Local Scour at Bridge Elements. *Journal of Hydraulic Engineering* 131 (2): 97–105. doi:10.1061/(ASCE)0733-9429(2005)131:2(97).

Salim, M., and J. S. Jones. 1996. Scour around exposed pile foundations. Proceedings of the North American Water and Environment Congress, ASCE, Anaheim, California, June 22–28.

Selamoglu, M., A. M. Yanmaz, and M. Koken. 2014. Temporal variation of scouring topography around dual bridge piers. In Proceedings of the Seventh International Conference on Scour and Erosion, Perth, Western Australia.

Sheppard, D. M., and R. Renna. 2010. *Florida Bridge Scour Manual.* Tallahassee, FL: Florida Department of Transportation.

Sheppard, D. M., B. Melville, and H. Demir. 2014. Evaluation of Existing Equations for Local Scour at Bridge Piers. *Journal of Hydraulic Engineering* 140 (1): 14–23. doi:10.1061/(ASCE)HY.1943-7900.0000800.

Tafarojnoruz, A., R. Gaudio, and F. Calomino. 2012. Evaluation of Flow-Altering Countermeasures against Bridge Pier Scour. *Journal of Hydraulic Engineering* 138 (3): 297–305. doi:10.1061/(ASCE)HY.1943-7900.0000512.

Tafarojnoruz, A., R. Gaudio, C. Grimaldi, and F. Calomino. 2010. Required conditions to achieve the maximum local scour depth at a circular pier. Proceeding XXXII Convegno Nazionale di Idraulica e Costruzioni Idrauliche, 14–17 September, Palermo, Italy, Farina, Palermo.

Tanaka, S., and M. Yano. 1967. Local scour around a circular cylinder. Proceeding of 12th IAHR Congress, International Association for Hydraulic Research, Delft, Netherlands, September 11–14.

Wang, H., H. Tang, Q. Liu, and Y. Wang. 2016. Local Scouring around Twin Bridge Piers in Open-Channel Flows. *Journal of Hydraulic Engineering* 142 (9): 06016008. doi:10.1061/(ASCE)HY.1943-7900.0001154.

Yilmaz, M., A. M. Yanmaz, and M. Koken. 2017. Clear-Water Scour Evolution at Dual Bridge Piers. *Canadian Journal of Civil Engineering* 44 (4): 298–307. doi:10.1139/cjce-2016-0053.

Zarrati, A. R., H. Gholami, and M. B. Mashahir. 2004. Application of Collar to Control Scouring around Rectangular Bridge Piers. *Journal of Hydraulic Research* 42 (1): 97–103. doi:10.1080/00221686.2004.9641188.

Zarrati, A. R., M. Nazariha, and M. B. Mashahir. 2006. Reduction of Local Scour in the Vicinity of Bridge Pier Groups Using Collars and Riprap. *Journal of Hydraulic Engineering* 132 (2): 154–162. doi:10.1061/(ASCE)0733-9429(2006)132:2(154).

Zhao, G., and D. M. Sheppard. 1999. The effect of flow skew angle on sediment scour near pile groups. Stream Stability and Scour at Highway Bridges. Papers Presented at Conferences Sponsored by the Water Resources Engineering (Hydraulics) Division of the American Society of Civil Engineers. ASCE.

Zokaei, M., A. R. Zarrati, S. A. Salamatian, and M. Karimaee Tabarestani. 2013. Study on Scouring around Bridge Piers Protected by Collar Using Low Density Sediment. *International Journal of Civil Engineering* 11: 199–205.